Biogeosciences Discuss., 12, 11423–11461, 2015
www.biogeosciences-discuss.net/12/11423/2015/
doi:10.5194/bgd-12-11423-2015

Biogeosciences Discussions
Open Access

Seagrass beds as ocean acidification refuges for mussels? High resolution measurements of pCO_2 and O_2 in a *Zostera marina* and *Mytilus edulis* mosaic habitat

V. Saderne[1], P. Fietzek[1,2], S. Aßmann[2], A. Körtzinger[1], and C. Hiebenthal[1]

[1]GEOMAR Helmholtz Centre for Ocean Research Kiel, Kiel, Germany
[2]Kongsberg Maritime Contros GmbH, Kiel, Germany

Received: 05 June 2015 – Accepted: 27 June 2015 – Published: 21 July 2015

Correspondence to: V. Saderne (vsaderne@geomar.de)

Published by Copernicus Publications on behalf of the European Geosciences Union.

Abstract

It has been speculated that macrophytes beds might act as a refuge for calcifiers from ocean acidification. In the shallow nearshores of the western Kiel Bay (Baltic Sea), mussel and seagrass beds are interlacing, forming a mosaic habitat. Naturally, the diverse physiological activities of seagrasses and mussels are affected by seawater carbonate chemistry and they locally modify it in return. Calcification by shellfishes is sensitive to seawater acidity; therefore the photosynthetic activity of seagrasses in confined shallow waters creates favorable chemical conditions to calcification at daytime but turn the habitat less favorable or even corrosive to shells at night. In contrast, mussel respiration releases CO_2, turning the environment more favorable for photosynthesis by adjacent seagrasses. At the end of summer, these dynamics are altered by the invasion of high pCO_2/low O_2 coming from the deep water of the Bay. However, it is in summer that mussel spats settle on the leaves of seagrasses until migrating to the permanent habitat where they will grow adult. These early life phases (larvae/spats) are considered as most sensitive with regard to seawater acidity. So far, the dynamics of CO_2 have never been continuously measured during this key period of the year, mostly due to the technological limitations. In this project we used a combination of state-of-the-art technologies and discrete sampling to obtain high-resolution time-series of pCO_2 and O_2 at the interface between a seagrass and a mussel patch in Kiel Bay in August and September 2013. From these, we derive the entire carbonate chemistry using statistical models. We found the monthly average pCO_2 more than 50 % (approx. 640 µatm for August and September) above atmospheric equilibrium right above the mussel patch together with large diel variations of pCO_2 within 24 h: 887 ± 331 µatm in August and 742 ± 281 µatm in September (mean ± SD). We observed important daily corrosiveness for calcium carbonates (Ω_{arag} and $\Omega_{calc} < 1$) centered on sunrise. On the positive side, the investigated habitat never suffered from hypoxia during the study period. We emphasize the need for more experiments on the impact of these acidic

conditions on (juvenile) mussels with a focus on the distinct day-night variations observed.

1 Introduction

Since preindustrial time, the atmospheric CO_2 mixing ratio rose from ~ 280 ppmv to actual 398.55 ppmv (Mauna Loa annual mean 2014, NOAA – ESRL). Future climate scenarios predict a strong further increase with one of them even approaching 1000 µatm by year 2100 (Caldeira and Wickett, 2005). The dissolution of increasing atmospheric CO_2 in seawater causes an increase in the seawater CO_2 partial pressure (pCO_2) and a concurrent decline of the seawater pH, a global phenomenon also referred to as ocean acidification (OA). Additively to OA, ocean warming and eutrophication of coastal waters worldwide cause a spreading and shoaling of hypoxia (< 60 µmol kg^{-1} O_2) in the ocean's interior (Diaz and Rosenberg, 2008; Keeling et al., 2010). These water masses regularly reach nearshore highly productive benthic habitats during wind driven upwelling events thereby contributing to the biogeochemical variability of coastal waters (Cai et al., 2011; Melzner et al., 2012; Saderne et al., 2013).

Both, hypoxia and OA can evoke severe consequences for marine fauna. Ocean acidification causes an increase of the corrosiveness of seawater against calcite and aragonite, the calcium carbonates composing the shells and skeletons of marine species (see Harvey et al., 2013; Andersson et al., 2011 for review and meta-analysis). Hypoxia generates a general down regulation of animal metabolism due to respiratory stress (Vaquer-Sunyer and Duarte, 2008). This metabolic depression is presumed to be reinforced under co-occurrence of OA and hypoxia (Pörtner, 2008; see discussion in Melzner et al., 2012).

A key but largely untested aspect of OA and/or hypoxia on fauna is the effect of periodic exposures to high pCO_2/low O_2 events (Andersson and Mackenzie, 2012; Duarte et al., 2013; Frieder et al., 2013). Especially nearshore habitats are exposed to this kind of important variations of CO_2 and O_2 caused by (seasonal) upwelling

events and the metabolism of the benthic flora and fauna. In highly vegetated habitats, photosynthesis and respiration of the plants and associated fauna drives important variations of pCO_2 and O_2 in the water column both on the diel and seasonal time scale (Hofmann et al., 2011; Saderne et al., 2013).

As an example, in Eckernförde Bay (western Baltic Sea) Saderne et al. (2013) found daily variations of pCO_2 of 200 to 400 µatm in summer in a macrophyte meadow dominated by the brown algae *Fucus serratus*, reaching up to 2200 µatm during upwelling conditions. As a consequence, seawater saturation states for calcite and aragonite (Ω_{calc} and Ω_{arag}) repeatedly fall for days below the dissolution threshold during such events ($\Omega = 1$).

Kiel Bay is in the south of Eckernförde Bay. Although geographically close, the nearshore habitats of both bays differ notably by the abundance of mussel beds on soft bottoms. While they are pervasive in Kiel Bay, they are almost absent in Eckernförde Bay (although abundant on hard substratum, Karez, 2008; V. Saderne et al., personal observation, 2011). As in several other enclosed bays of the western Baltic Sea (Vinther et al., 2012), the mussel *Mytilus edulis* and seagrass *Zostera marina* co-occur in patches forming a mosaic habitat (Reusch and Chapman, 1995; Vinther et al., 2008, 2012; Vinther and Holmer, 2008).

In an harbor of Kiel Bay, Thomsen et al. (2010) have shown that mussel recruitment occurs in July and August, a period of the year during which CO_2 partial pressures exceeding 1000 µatm were measured close by. In the soft bottom nearshore environment of the Baltic Sea, seagrass beds act as a larval trap for mussels (Reusch, 1994, 1998). Mussel larvae are known to massively use seagrass shoots as substratum for their primary settlement (Bologna et al., 2005; Herkül and Kotta, 2009) and to migrate with currents to a secondary settlement area using a modified byssal thread as a sail (Newell et al., 2010 and references therein). In Kiel Bay, shoots of *Zostera marina* fully covered by mussel spats can be observed in July/August (personal observation, 2013) presumably before settling definitely in adjacent mussel beds or patches within the seagrass bed (Reusch, 1994, 1998). They must then reach the "refuge" size of

~ 30–50 mm (> 1 year old) above which mussels cease to be predated by seastars *Asteria rubens* and shore crabs *Carcinus maenas* (Reusch and Chapman, 1997; Sommer et al., 1999; Enderlein et al., 2003).

During these critical first months post recruitment, freshly arrived mussels on the patch are exposed to important variations of O_2 and carbonate chemistry. In such vegetated habitats, daytime photosynthesis has the potential to offer a refuge to OA to larval and juvenile stages. Oppositely at night, OA effects could be reinforced by respiration. Frieder et al. (2013) showed that the negative effects of elevated pCO_2 (~ 1500–1600 µatm) on larvae of *Mytilus galloprovincialis* disappear, if diel variations of 500 µatm were added, although this was not observed for the larvae of *Mytilus californianus*. However, the magnitude and temporal extend of these short frequency variations (hours to days) in the seagrass beds are unknown for the Baltic among other water bodies. Likewise the evolution of these variations in the context of ocean acidification and deoxygenation deserve increased investigations.

In the present study, we investigate the variations of O_2 and carbonate parameters pCO_2, total dissolved inorganic carbon (DIC), total alkalinity (TA), pH, $\Omega_{aragonite}$ and $\Omega_{calcite}$ that the mussels have to endure during their first summer in the seagrass meadow due to meadow metabolism and up- and downwelling events. We used a combination of autonomous in-situ sensors for pCO_2, O_2, salinity and temperature as well as discrete sampling for DIC and alkalinity for a period of more than 7 weeks in summer 2013.

2 Materials and methods

2.1 The site

Mixed benthic communities structured by the seagrass *Zostera marina* and the mussel *Mytilus edulis* form typical mosaic habitats on sandy nearshore bottoms of the western Baltic Sea.

The sensor package measuring pCO_2, O_2, salinity and temperature was deployed at 2 m depth in a mixed habitat formed by the seagrass *Zostera marina* and the mussel *Mytilus edulis* in Kiel Bay, western Baltic Sea (54°20′48″ N, 10°09′14″ E; see Fig. 1). The sensor was directly placed on a mussel patch within the seagrass bed. The deployment was conducted for 50 days from the 08 August 2013 to 27 September 2013 with short power interruptions form 10 August 2013 17:10 LT to 11 August 08:00 LT and from 12 August 05:00 LT to 14 August 16:00 LT.

2.2 In situ sensor suite

Temperature, salinity and O_2 were measured simultaneously every 10 min with a SBE 37–SI (temperature and salinity, Sea-Bird electronic Inc., USA) and an oxygen optode Aanderaa 3835 (Aanderaa Data Instruments AS, Norway) enclosed in a flow cell. The sensors were recently purchased and their specs are supposed to meet the manufacturer's data. The circulation of water between the SBE 37–SI and the optode is achieved by a SBE 5M pump (Sea.-Bird electronic Inc., USA), that ran for 30 s every 10 min. The coordination of pumping and recording by the SBE 37 and the optode is carried out by a custom-made data logger. To prevent fouling on sensors, the SBE 37–SI was equipped with tributyltin tablets and copper tubing linked the SBE 37–SI and the flow cell to the pump.

A HydroC™ CO_2 II (KM Contros GmbH, Kiel, Germany) was used to measure pCO_2 with 1 min interval. The HydroC™ determines the CO_2 partial pressure (pCO_2) optically by means of an NDIR absorption measurement within a membrane-equilibrated headspace (Fietzek et al., 2014). The sensor was calibrated at a water temperature of 17.5 °C across a measurements range of 200–2200 µatm by the manufacturer before (June) and after (November) the measurements. Calibrations and data processing were carried out according to Fietzek et al. (2014). During the processing, information from the two calibrations as well as from the regular zeroings during the deployment was used to enhance data quality. For this, the transformation of the pre- into the post-

deployment calibration polynomial was carried out according to the sensors absolute run-time between the two calibrations.

During the field deployment, the sensor was provided with power from the nearby pier. Data were stored internally on its data logger. The sensor was configured to carry out a 2 min zeroing every 6 h. The flush interval used to flag the data during recovery from zero to ambient values was set to 15 min. During the subsequent measure interval a 10 s mean of the 1 Hz raw data was stored every minute.

The HydroC™ was equipped with a flow-through cell in front of the membrane as well as with a water pump, which was deactivated during the deployment. By that, a disturbance of the benthic boundary layer through constant pumping was avoided (Although disturbance by the SBE 5M pump every 10 min could not be avoided). The sensor's response time (RT) and especially the related signal processing therefore had to be given special attention (see the Appendix for further information). The un-pumped sensor's RT was determined to be 292 ± 64 s (mean ± SD) and the pCO_2 series was therefore response time corrected assuming a constant RT of 292 s. In order to estimate the overall uncertainty in the pCO_2 measurement caused by the longer RT aspect, the data were additionally response time corrected once with a constant minimum RT of $RT_{min} = 292–64$ s, and once with a maximum RT of $RT_{max} = 292 + 64$ s. Subtraction of the data corrected with an assumed RT_{max} from the data corrected assuming the RT_{min} yields an average ΔpCO_2 of −0.5 µatm and a corresponding standard deviation of 6.8 µatm. Considering also the general uncertainty of drift corrected HydroC™ pCO_2 data (±0.5 % of the upper range value) and the potentially strong effect of varying water exchange in front of the membrane, we conservatively estimate the final uncertainty in the pCO_2 data with unpumped flow-through cell configuration to be ±30 µatm for the measurements described here.

2.3 Discrete sampling

Over the course of the deployment, a total of 31 seawater samples for DIC and TA were taken close to the sensor suite while snorkeling. Sampling was conducted at the

sensor suite twice a week in the hour following sunrise and solar noon. On a third day, duplicate sampling was conducted in the hour following solar noon. Corresponding sampling results were averaged to improve the quality of the measurements. In parallel to all DIC and TA samplings, seawater was sampled and frozen for measurement of ammonium, nitrate, nitrite, phosphate and silicate concentrations. Back in the lab, the salinity of the samples for DIC and TA was measured using a conductometer (SG 7/8, Mettler Toledo, Switzerland) and the samples were poisoned with mercury chloride following Dickson (2007).

DIC was measured by coulometry using a SOMMA instrument (University of Rhode Island, USA) and total alkalinity was determined with a VINDTA titrator (Marianda GmbH, Germany) following Dickson (2007).

Ammonium, nitrite, nitrate, phosphate and silicate concentrations were measured using a QuAAtro autoanalyzer with an XY-2 sampler (SEAL Analytical GmbH, Germany) in a total number of 31 samples.

2.4 Seawater carbonate chemistry

We used a model approach to estimate total alkalinity from salinity. Given the obvious changes particular in phosphate and salinity around 01 September (Fig. 4), two separate alkalinity–salinity regressions were calculated for August and September (Fig. 6, Table 2).The slope and intercept were used to transform the salinity time series from the SBE-37 into a series of total alkalinity. Both regressions were highly significant with p values < 0.001 and standard deviations of the residuals < 15 µmol kg^{-1}. The two intercepts for August and September are notably differing by 100 µmol kg^{-1} while both slopes being rather similar (∼ 40 µmol kg^{-1} psu^{-1}). Temperature and salinity were used together with the pCO_2 time series of the HydroC™ and the modelled total alkalinity series as input parameters to the carbonate system calculations. Calculations were carried out with the R package Seacarb (Lavigne and Gattuso, 2013) using first and second carbonate system dissociation constants for estuarine systems from Millero

(2010) and the dissociations constants of HF and HSO4- of Perez and Fraga (1987) and Dickson (1990) respectively

2.5 Community metabolism

We used the method of the open mass balance of O_2 (Odum, 1956) to calculate the gross primary production (GPP), net primary production (NPP) and community respiration (CR) (net community production (NCP) = gross community production (GCP) – CR) of the seagrass/mussel mixed habitat as in Champenois and Borges (2012). This method allows a semi quantitative, habitat integrative estimation of the production and consumption of O_2 due to the habitat (plants and animal's respiration and photosynthesis respectively, Gazeau et al., 2005; Champenois and Borges, 2012). Fluxes of O_2 at every sampling time t were calculated as the difference between O_2 at t and the previous O_2 at $t - 10$ min. GPP is calculated as the sum of the fluxes of O_2 during daytime after correction for the air–sea exchanges of O_2. Reciprocally, CR is the sum at nighttime, after air sea exchange of O_2. Air sea exchange of O_2 (transfer velocity in $m\,s^{-1}$) is calculated from wind speed at 10 m with the R package Marelac (Soetaert et al., 2012) using the method and parameterization of Nightingale et al., 2000. Daytime and nighttime (irradiance = $0\,W\,m^{-2}$) duration as well as wind speed were obtained from instruments at the top of the GEOMAR west shore building, 2 km south from the experimental site.

2.6 Calculation of the regional atmospheric pCO_2

Dry atmospheric CO_2 mole fractions from Umweltbundesamt, Station Westerland, location: 8.308208° E and 54.924967° N, were averaged for the months August (08–31 August 2013) and September (01–27 September 2013). Thereof pCO_2 in wet air (100 % relative humidity) of 385 and 387 µatm for August and September respectively were derived at local measurement conditions; i.e. using an averaged sea surface temperature and ambient pressure readings (both GEOMAR meteorological station) as well as the salinity measured in this study.

3 Results

The time-series of dissolved oxygen and pCO_2 are shown in Figs. 2 and 3, respectively. Daily means, maximums, minimums and day-night peak-to-peak amplitudes (mean ± SD) are presented in Table 1 for the months of August and September. The data from the discrete sample nutrient measurements as well as the temperature and salinity series are depicted in Fig. 4.

The daily mean O_2 concentration most of the time remains below the seawater saturation threshold (approx. 260 to 290 $\mu mol\,O_2\,kg^{-1}$) for the two months of August and September. In August, supersaturation due to dominance of photosynthesis is regularly observed between noon and sunset. A significant decrease of the daily average O_2 concentrations by 47 $\mu mol\,kg^{-1}$ can be observed in September with an important step occurring on 08 September in parallel to a sudden decrease in temperature by approx. 2 °C. In the subsequent period, mean, maximum and minimum O_2 concentrations are almost entirely below saturation (see Table 1). A slight decrease of the day-night amplitude by 29 $\mu mol\,kg^{-1}$ is observed from August to September. An O_2 concentration of 60 $\mu mol\,kg^{-1}$ O_2, considered as the threshold for hypoxia is never reached; the minimum concentration observed during the two months was of 140 $\mu mol\,k^{-1}$ (see Fig. 2).

A mean decrease of NPP of 38.4 $mmol\,O_2\,m^2\,d^{-1}$ was calculated between August and September, due to a mean increase of the CR by 24.4 $mmol\,O_2\,m^2\,d^{-1}$ and a mean decrease of GPP by 10.5 $mmol\,O_2\,m^2\,d^{-1}$ (see Fig. 5).

Over the entire measurement period, the daily mean pCO_2 remained always above the regional atmospheric pCO_2 of approx. 386 µatm. As opposed to O_2, a modest increase of the daily means was observed between August and September (+21 µatm) as well as an average decrease of the day-night variability by 143 µatm (see Table 1).

A high pCO_2 event was observed between 08 and 12 September with a peak of the daily mean pCO_2 to 1173 µatm on 09 September. This day, a maximum pCO_2 of 1863 µatm was observed at 4:30 a.m. (see Fig. 3).

The TA time series was modeled from the salinity time series using the parameters of a TA to salinity relationship establish on the measurements of discrete samples (Fig. 6). We were not able to distinguish any calcification effect on TA. More specifically, no systematic increase or decrease of alkalinity was found between sunrise and noon sampling. The average calculated TA for the entire measurement period was 1962 ± 40 (mean ± SD) µmol kg^{-1}, with a noticeable increase to a maximum of 2031 µmol kg^{-1} between 28 August and 02 September followed by a rapid decrease to a minimum of 1840 µmol kg^{-1} between 02 September and 09 September (Fig. 6).

Calculated times series for DIC, pH and Ω_{arag} and Ω_{calc} (Fig. 7) were analyzed for daily means, minima, maxima and diel peak-to-peak amplitudes (mean ± SD) (Tables 1 and 3). Overall we observe a slight decrease in daily means of DIC and pH between August and September by 14 µmol kg^{-1} and 0.023 pH units respectively. In parallel, we observe a decrease of the amplitudes of the diel variations in DIC and pH of 37 µmol kg^{-1} and 0.09 pH units. All these observations are coherent with the changes in pCO_2 previously described. The high pCO_2 event of 09 September translates into a minimum daily mean pH values of 7.653. The low alkalinity event around 06 September does not have a noticeable effect on pH, pCO_2 or the saturation states Ω_{arag} and Ω_{calc} as it was associated with an similarly strong decrease of DIC down to a minimum daily mean of 1747 µmol kg^{-1}.

Daily means of Ω_{arag} are close to the saturation threshold: 1.4 in August and 1.2 in September. For both, Ω_{arag} and Ω_{calc}, we observe a decrease in daily mean values and diel amplitudes between August and September (see Table 3). The amplitude decrease results from a reduction of the daily maximum with the minima remaining constant for both isoforms. On average, the seawater is undersaturated with respect to Ω_{arag} for 5.7 ± 4.0 h d^{-1} in August and 8.8 ± 6.3 h d^{-1} in September. Similarly, seawater is undersaturated with respect to calcite for 0.4 ± 0.8 h d^{-1} and 1.3 ± 2.4 h d^{-1} in August and

September, respectively. Only one full day of undersaturation with respect to aragonite was observed on 09 September at the apogee of the high pCO_2 event.

4 Discussion

The pCO_2 calculated from DIC and TA measurements on the discrete samples, $pCO_{2,calc}$, and pCO_2 measured by the HydroC™, $pCO_{2,meas}$, show certain characteristics and inconsistencies. The difference of $pCO_{2,meas}$ and $pCO_{2,calc}$ is rather variable and a function of $pCO_{2,meas}$ (Fig. 8).

Similar comparisons between the directly measured carbonate system variable on the discrete samples, TA_{meas} and DIC_{meas}, and the values derived from the corresponding other two parameters (DIC_{meas} and $pCO_{2,meas}$ as well as TA_{meas} and $pCO_{2,meas}$ respectively) are characterized by large variability as well (mean ± SD): TA_{meas} minus $TA_{calc,DIC\text{-}pCO_2}$ is 9.5 ± 28.0 µmol kg^{-1} and DIC_{meas} minus $DIC_{calc,TA\text{-}pCO_2}$ is -9.3 ± 25.8 µmol kg^{-1}. The high pCO_2 disagreement at high $pCO_{2,meas}$ (Fig. 8) corresponds clearly to high TA and low DIC values. If $TA_{meas} - TA_{calc,DIC\text{-}pCO_2}$ and $DIC_{meas} - DIC_{calc,TA\text{-}pCO_2}$ are plotted as a function of TA_{meas} and DIC_{meas}, respectively, no such clear trend was found as seen for pCO_2.

A potential bias within CO_2 system calculations can originate from TA determinations in low salinity waters. Our TA analyzer is not tailored to measurements in brackish waters. Thus, we ran an intercomparison between our set up and the one used at Leibniz Institute for Baltic Sea Research in Warnemünde (IOW) specifically for Baltic sea samples (open cell analyzer as described in SOP 3b, Dickson et al., 2007). Based on the analysis of 6 discrete water samples from Kiel Bight taken at GEOMAR (Fig. 1), we found that the measurements on the analyzer used for this study were too low by 7.5 ± 3.2 µmol kg^{-1} (mean ± SD). Despite such a likely salinity dependent bias, this offset does not explain the characteristics found within the pCO_2 comparison.

Another potential source of error, especially with coastal carbonate system calculations, involves organic alkalinity contributions. Organic molecules can increase the buffering capacity of sea water, what can erroneously be interpreted as part of the carbonate alkalinity during titration (Kuliński et al., 2014). The 6 duplicate samples were therefore also analyzed for DIC (SOMMA instrument, University of Rhode Island, USA) and pH (cf. Hammer et al., 2014). From this, a mean difference (± SD) between TA_{meas} and $TA_{calc,DIC\text{-}pH}$ of 26.7 ± 2.4 µmol kg^{-1} was found. A potential effect of sample storage duration (in this case ∼ 9 month) as well as of poisoning on the determined TA_{org} could not be quantified. However this difference provides a general indication for a significant TA_{org} contribution in Kiel bight (Kuliński et al., 2014). Although a TA correction for this TA_{org} contribution would shift the observed pCO_2 characteristics in the right direction, it would not explain the observed inconsistency at elevated pCO_2 levels, since TA_{org} is expected to become smaller with decreasing pH/increasing pCO_2 (the smaller the pH, the larger is the abundant fraction of TA_{org} in protonated form and therefore the smaller is the TA_{org} effects during the titration). Figure 8 shows an opposing behavior.

The effects of low salinity on TA determination and the TA_{org} influence are of opposing sign and were not considered in the calculations. However these are of significant relevance for coastal carbonate system determinations. Using a smaller TA in CO_2 system calculations leads to lower pH values or higher pCO_2. Importantly, not considering a potential TA_{org} contribution in our study, causes carbonate system determinations to be conservative estimates in an OA context. Not subtracting an organic fraction from the measured alkalinity leads to overestimation of TA and hence lower $pCO_{2,calc}$ and higher pH_{calc} as well as higher calculated saturation states.

Beside the low salinity effect and a potential TA_{org} contribution, the fact that a linear fit to the TAsalinityrelationship shows a better R^2 for TA_{meas} than for $TA_{calc,DIC\text{-}pCO_2}$ indicates that the observed characteristics depicted in Fig. 8 relate to either pCO_2 or DIC rather than to the TA measurements.

The variability observed in the $pCO_{2,meas} - pCO_{2,calc}$ is much larger than the ±30 µatm uncertainty estimated for the HydroC™ measurements under the conditions

of this study. The observed discrepancy at elevated pCO_2's (Fig. 8) would correspond to an unrealistic measurement uncertainty of ∼ 50 %. This is extremely unlikely since the sensor successfully passed calibration in the range of 200–2200 µatm before and after the deployment with the sensor's pCO_2 dependent behavior remaining sufficiently similar.

We therefore attribute the observed discrepancies between measured and calculated pCO_2 to strong pCO_2 gradients on small spatial scale near the mussel bed. The unpumped pCO_2 sensor rested directly on the mussel patch with the membrane being only 5–10 cm above ground while the discrete samples were taken at a distance of ∼ 2030 cm from the sea floor. We therefore decided to use the pCO_2 time series as measured without any corrections and the derived TA-S time series for the carbonate system calculations. Being (quasi-) conservative quantities and far less susceptible to biological perturbations, TA and salinity are less prone to the development of strong local gradients. The fact that provision of water to the CO_2 sensor's membrane in this particular experiment relied on currents and diffusion rather than pumping (as in typical applications of the HydroC™ sensor), would at maximum have caused a smoothing of the signal but neither a systematic and pCO_2-dependent offset nor further increased observed daily variations. As described in the Appendix, response time effects were corrected very carefully, and we are confident with the given pCO_2 uncertainty.

The monthly averages of pCO_2 close to the seafloor as presented in this study (∼ 640 µatm; Table 1) are more than 50 % above atmospheric pCO_2. In 2011, Saderne et al. (2013), using the same technologies in a seaweed dominated bed of Eckernförde Bay (adjacent to Kiel Bay in the western Baltic) found weekly mean pCO_2 values of ∼ 390 µatm in July, ∼ 240 µatm in August and 420 µatm in September (without including an upwelling event). We explain the high pCO_2 of this study by the respiratory activity of the mussels and the sediment directly beneath the sensor's membrane.

Accordingly, the day-night amplitudes observed in the present study are 3 to 4 time higher than observed by Saderne et al. (2013). In Eckernförde Bay in 2011, the pCO_2 mean and variations (∼ 1600 and ∼ 1700 µatm, respectively,) were only higher during

a September upwelling event, with the invasion of salty, low-pH water from depth to the nearshore area. DIC variations driven by net biological activity have a stronger effect on pCO_2 at high pCO_2, because of a reduced buffering capacity of the carbonate system and a reduced speciation of the dissolved CO_2. Therefore the extreme pCO_2 variations induced by plant photosynthesis observed in 2011 are the consequence of the increased baseline pCO_2 due to the upwelling. The fact that DIC variations were actually reduced, highlight a reduction of photosynthesis albeit the extreme pCO_2 variations observed. Assuming respiration of mussels not to be time dependent the same effect of an elevated pCO_2 level as in an upwelling scenario would also explain a shift of the weekly mean pCO_2 towards higher values (~ 640 µatm) as observed in this study.

A similar mechanism might constantly occur right above a mussel patch surrounded by seagrass. The mussel respiration increases the pCO_2 baseline, inducing a shift in the carbonate system speciation amplifying the CO_2 variations due to photosynthesis. This is attested by the fact that although the diel pCO_2 variations are extreme in the present study, the amplitude of the diel DIC variations – reflecting the net community production at this site – are in agreement with what had been observed in Eckernförde Bay before and after upwelling 141 and 106 µmol kg^{-1} respectively (Saderne et al., 2013) vs. 166 µmol kg^{-1} in August and 129 µmol kg^{-1} in September in the present study.

The O_2 sensor inlet was ~ 30 cm above ground (mussels) and equipped with a pumping system sampling every 10 min. We expect less strong impact of the mussels' respiration and the measure being less driven by local near-sediment-surface phenomena. Still, the mean O_2 found is significantly below saturation, with an important decrease occurring in September (monthly means of 89.4 % O_{2sat} and 68.8 % O_{2sat} found in August and September respectively). In parallel to this study, Schneider et al. (2015) have measured O_2 in 5 seagrass patches without mussels on a northern position in Kiel Bay (Kiel-Holtenau, 54°22′29″ N; 10°09′35″ E). Compared to our study they measured O_2 being elevated by 54.0 ± 14.7 µmol kg^{-1} (mean ± SD, n = 3 days of comparison) in August and 99.7 ± 22.8 µmol kg^{-1} in September (mean ± SD, n = 6 days of comparison).

As for the high pCO_2 values, the low concentrations of O_2 in our study can be explained by the mussels' respiration.

Altogether, we observe a decrease of dissolved oxygen, an increase of the mean pCO_2, a decrease of the diel DIC variations and an increase of total phosphate between August and September. In addition, the amplitudes of both daily O_2 and pCO_2 variation become smaller (see Table 1). All this is consistent with the decrease in net primary production observed and the visual perception of a progressive degradation of the seagrass shouts, as the mosaic habitat is turning heterotrophic from August to September. However, we note that at no point of our survey the threshold of hypoxia (60 µmol kg^{-1}) was reached, principally because of the lack of a major upwelling event in early fall 2013. For comparison, Fig. 9 is displaying an upwelling event for the same period in 2014, recorded at 1 m depth at the GEOMAR pier mooring with the exact same sensors as in this study. Then, surface water fringed hypoxia and the pCO_2 reached > 2000 µatm. These already extreme conditions might have been even more prominent within the mosaic habitats, when superimposed mussel respiration and the diel variations due to photosynthesis and respiration of seagrass.

Seagrass is known to be very intolerant to oxygen deprivation (see e.g. Holmer and Bondgaard, 2001; Raun and Borum, 2013), this sensitivity being amplified at warm temperatures (Raun and Borum, 2013). Low oxygenation leads to suffocation of the shoot meristems and sulfide poisoning of the rhizomes and roots, forcing the seagrass to switch to anaerobic metabolism (Holmer and Bondgaard, 2001). Seagrass can benefit of the cohabitation with mussel through e.g. clearance of water and ammonia excretion (Peterson and Heck, 2001; see Vinther et al., 2008 for review). However, if too abundant, mussels can exclude seagrass, due to the hypoxic and sulfidic stress caused by mussel respiration and feces/pseudo-feces accumulation (Vinther et al., 2012, 2008). Dolmer et al. (2009) found in the Little Belt Danish strait a threshold of 1.6 kg mussel m^{-2} above which seagrass beds are excluded (Vinther et al., 2012). For Flensburg Bay (German Baltic Sea, north to Kiel Bay and Eckernförde Bay), Vinther et al. (2008) conclude that the cohabitation of mussels and seagrass is mostly to the

detriment of the latter. Yet, in contrast with the reduced O_2, the respiratory CO_2 of the mussels (or upwelling) could be beneficial to the seagrass. Seagrass are known to be CO_2 limited in present sea, a possible heritage of a photosynthetic metabolism adapted to the high CO_2 of the Cretaceous that saw them appear (Beer and Koch, 1996; Invers et al., 1997). However, on the few studies existing to date, there is no convincing evidence of long term fertilization effect of elevated CO_2 on seagrass (see Garrard and Beaumont, 2014 for review).

Mytilus edulis is an euryoxic bivalve (Wang et al., 1992; Wang and Widdows, 1993) and we do not expect the minimal O_2 reached in our survey (140 µmol kg^{-1}) to be of any detrimental consequences to it. Contrastingly, the O_2 during an upwelling event such as shown in Fig. 9 in a mosaic habitat might affect mussel metabolism. Prolonged hypoxia (> 2 days at ≤ 60 µmol O_2 kg^{-1}) has shown to cause reduction in feeding and growth rates (Wang and Widdows, 1993; Sanders et al., 2014) and to cause a partial switch to anaerobic metabolism (Wang and Widdows, 1993). During upwelling events, the mussels may experience enhanced hypoxia during night and also hypoxic stress relaxation during day because of the superimposition of respiration and photosynthesis to low oxygen upwelled water (unless impairment of the seagrass physiology by hypoxia). We found very important variations of Ω_{calc} and Ω_{arag} on a daily basis with 5.7 to 8.8 h of undersaturation for aragonite per day in the water body right above the mussel patch. Waldbusser et al. (2014) demonstrated that saturation states, (and so $[CO_3^{2-}]$) are the only parameters affecting the larval development and growth of *M. Galloprovincialis* and *Crassostrea gigas* and not pH or CO_2. On young *M. edulis* Hiebenthal et al. (2013) found a negative correlation between growth and $\Omega/[CO_3^{2-}]$. On a new study, Thomsen et al. (2015) confirmed these findings in larvae and juveniles. With a meta-analysis including all past work on mussel populations from Kiel Bay, they found that the critical CO_3^{2-} concentration below which calcification starts to decline was 80 µmol kg^{-1} (although they specified that the confounding ratio H^+/HCO_3^- is likely to be the effective parameter for calcification). With mean $[CO_3^{2-}]$ of 75 and 87 µmol kg^{-1} in August and September (Table 1, Fig. 10), respectively, in our survey, mussels were exposed

for most of the day to $[CO_3^{2-}]$ below this threshold. On the other hand, our experimental mussel patch experiences important oscillations around this rather low mean $[CO_3^{2-}]/\Omega$ on daily basis. The consequence of these successions of intense acidic stress and stress relaxation on the juvenile and adults forming the mussel patch is so far unknown. Furthermore, Thomsen et al. (2014) showed that high food availability, particularly in Kiel Bay, can circumvent the effects of acidification in mussels.

5 Conclusion

In this study, we investigated the variations of O_2 and carbonate parameters pCO_2, DIC, total alkalinity, pH, Ω_{arag} and $\Omega_{calcite}$ directly on a mussel patch within a seagrass meadow of Kiel Bay for more than 7 weeks in summer 2013. The analysis is based on field data from a combination of autonomous in-situ sensors for pCO_2, O_2, salinity and temperature as well as from discrete sampling for DIC and alkalinity as well as phosphate and silicate. We highlight that carbonate system observation in benthic habitats is challenging and complex due to the high temporal and spatial variability at very small spatial scale.

Previous investigations already highlighted the low pH of Baltic waters (e.g. Tyrrell et al., 2008). The mussels living in the mosaic seagrass/mussel habitats experience even higher acidification and very important daily fluctuations. We found 5.7 to 8.8 h of corrosive Ω_{arag} per day above the mussel patch. The threshold of $[CO_3^{2-}]$ below which calcification is impacted in mussel as identified by Thomsen et al. (2015) of 80 µmol kg^{-1} is also exceeded most of the day.

It is unknown how these will react to the global increase of atmospheric values, how mussels cope with these fluctuations and if these are beneficial or detrimental to mussels, spats and juveniles/adults. On top of it lies the question whether seagrass beds could be refuges for mussels in a context of future OA. The abundance of mussels in Kiel Bay, despite the prevailing high pCO_2 levels, are a positive sign that mussels might

survive OA worldwide, however the future of mussels in Kiel Bay is more uncertain, if OA superimposes to the present high pCO_2 (as assumed in Melzner et al., 2012).

Our study demonstrates how essential and valuable it is to place more effort in measuring the carbonate chemistry variations in nearshores habitats, and the need to go beyond the relatively low and stable open ocean values and predictions in OA research on the ecology of benthic organisms. Our study also points at the fact that due to small scale spatial variability a combined autonomous and manual measurement/sampling approach has to be designed with particular attention to the exact sampling spot. Only truly co-located sampling by autonomous and manual techniques will assure good comparability of the results.

Appendix: HydroC™ response time and related signal processing

Fitting a first order kinetics model to the HydroC™'s signal recovery from its zero value to ambient partial pressure over the 15 min flush interval data (see Fiedler et al., 2013) provides response times of 414 ± 119 s with an average fit error of 4.2 ± 1.7 s from the total of 190 flush intervals conducted during the deployment. In general the carbonate system at the site was characterized by a strongly varying baseline featuring very steep pCO_2 gradients over the course of the day with slopes of up to ∼ 100 µatm per 17 min (i.e. 1020 s). Therefore the pCO_2 signal recovery from zero to ambient during the flush intervals was always superimposed with a changing background partial pressure. These adverse conditions hamper and bias the response time determination by means of a first order kinetics fit. We therefore applied a response time model, which additionally comprises a linear component in addition to the exponential response time related signal recovery. With an average response time of 242 ± 105 s and the corresponding average fit error of 9.8 ± 11.4 s the obtained response times are generally much shorter, which relates to the fact that the fit erroneously tends to attribute too much signal change to the linear component in order to best align the fit to the input data. Our best response time determinations would therefore be found in situations in

which there was the smallest background pCO_2 change over the course of the flush interval. As a first step to help within this focusing we only proceeded with the flush intervals whose response times determined by the simple and the extended signal model differed by less than 30 s from each other. From this set we then visually selected only the flush intervals throughout which the pCO_2 background signal changed by less than 30 µatm. The final selection comprised 8 response times averaging to 292 ± 64 s with an average fit error of 3.3 ± 0.8 s.

Still, the standard deviation of the response times is comparably large. We attribute this to the fact that the derived response time depends on the flow conditions in front of the membrane which were neither controlled nor constant during the deployment. Furthermore, the determined response time relates to the CO_2 transport process from the water body in front of the membrane through the semi-permeable layer into the internal gas circuit. It does not necessarily comprise the time required for the water exchange between the volume in front of the membrane and the surrounding water. This exchange was impeded by the installed flow head and water pump. The large variability of the determined response time and the uncertainty related to the dynamics of the water exchange mark the largest uncertainties related to the pCO_2 measurements. Against this background, a temperature dependence of the response time can be neglected as well as a deceleration caused by fouling on the membrane, which was only observed to a very small extend. Therefore the response time correction according to Miloshevich et al. (2004) and Fiedler et al. (2013) was carried out with a constant response time of 292 s.

Acknowledgements. The authors would like to thank particularly Todd Martz and his team from the Scripps Institution of Oceanography (San Diego, USA) for providing the salinity/O_2/T° sensor package and for their precious technical assistance. We also wish to thank the Kiel Marine Organism Culture Centre (KIMOCC) of the Kiel Cluster of excellence "Future Ocean"; Sebastian Fessler from GEOMAR for the TA/DIC sample measurements; Bernd Schneider and Stefan Bücker from the IOW are thanked for valuable discussions with respect to carbonate system analysis in the Baltic Sea as well as for the inter comparison between TA/DIC/pH measurements; Peter Herman from the NIOZ Royal Netherlands Institute for Sea Research for

providing access to the nutrient analyzer; Jörn Thomsen for his comments on the manuscript; the research divers from GEOMAR among which Martin Wahl, Christian Pansch, Yvonne Sawall and Christian Lieberum; the personnel of the "Seebar am Seebad Düsternbrook" restaurant for providing electricity to the sensors as well as the Kiel early morning nudist club for its cooperation. This work has been funded by the Kiel Cluster of excellence "Future Ocean".

The article processing charges for this open-access publication were covered by a Research Centre of the Helmholtz Association.

References

Andersson, A. J. and Mackenzie, F. T.: Revisiting four scientific debates in ocean acidification research, Biogeosciences, 9, 893–905, doi:10.5194/bg-9-893-2012, 2012.

Andersson, A. J., Mackenzie, F. T., and Gattuso, J.-P.: Effects of ocean acidification on benthic processes, organisms, and ecosystems, in: Ocean Acidification, Oxford England; New York: Oxford University Press, xix, 326 pp., 2011.

Beer, S. and Koch, E.: Photosynthesis of marine macroalgae and seagrass in globally changing CO_2 environments, Mar. Ecol.-Prog. Ser., 141, 199–204, doi:10.3354/meps141199, 1996.

Bologna, P. A. X., Fetzer, M. L., McDonnell, S., and Moody, E. M.: Assessing the potential benthic–pelagic coupling in episodic blue mussel (*Mytilus edulis*) settlement events within eelgrass (*Zostera marina*) communities, J. Exp. Mar. Biol. Ecol., 316, 117–131, doi:10.1016/j.jembe.2004.10.009, 2005.

Cai, W.-J., Hu, X., Huang, W.-J., Murrell, M. C., Lehrter, J. C., Lohrenz, S. E., Chou, W.-C., Zhai, W., Hollibaugh, J. T., Wang, Y., Zhao, P., Guo, X., Gundersen, K., Dai, M., and Gong, G.-C.: Acidification of subsurface coastal waters enhanced by eutrophication, Nat. Geosci., 4, 766–770, doi:10.1038/ngeo1297, 2011.

Caldeira, K. and Wickett, M. E.: Ocean model predictions of chemistry changes from carbon dioxide emissions to the atmosphere and ocean, J. Geophys. Res., 110, 1–12, doi:10.1007/s00227-012-1954-1, 2005.

Champenois, W. and Borges, A. V.: Seasonal and interannual variations of community metabolism rates of a *Posidonia oceanica* seagrass meadow, Limnol. Oceanogr., 57, 347–361, 2012.

Diaz, R. J. and Rosenberg, R.: Spreading dead zones and consequences for marine ecosystems, Science, 321, 926–929, doi:10.1126/science.1156401, 2008.

Dickson, A. G.: Standard potential of the reaction: $AgCl(s) + 1/2\,H_2(g) = Ag(s) + HCl(aq)$, and the standard acidity constant of the ion HSO_4^- in synthetic sea water from 273.15 to 318.15 K, J. Chem. Thermodyn., 22, 113–127, doi:10.1016/0021-9614(90)90074-Z, 1990.

Dickson, A. G., Sabine, C. L., and Christian, J. R. (Eds.): Guide to Best Practices for Ocean CO_2 Measurements, PICES spec., Special Publication 3, 191 pp., 2007.

Dolmer, P., Christoffersen, M., Geitner, K., and Kristensen, S.: Konsekvensvurdering af fiskeri på blåmuslinger i Lillebælt 2008/2009 Maj 2009, DTU Aqua-rapport nr. 213, Charlottenlund, Institut for Akvatiske Ressourcer, Danmarks Tekniske Universitet, 67 pp., 2009.

Duarte, C. M., Hendriks, I. E., Moore, T. S., Olsen, Y. S., Steckbauer, A., Ramajo, L., Carstensen, J., Trotter, J. A., and McCulloch, M.: Is ocean acidification an open-ocean syndrome? Understanding anthropogenic impacts on seawater pH, Estuar. Coast., 36, 221–236, doi:10.1007/s12237-013-9594-3, 2013.

Enderlein, P., Moorthi, S., Röhrscheidt, H., and Wahl, M.: Optimal foraging vs. shared doom effects: interactive influence of mussel size and epibiosis on predator preference, J. Exp. Mar. Biol. Ecol., 292, 231–242, doi:10.1016/S0022-0981(03)00199-0, 2003.

Fiedler, B., Fietzek, P., Vieira, N., Silva, P., Bittig, H. C., and Körtzinger, A.: In situ CO_2 and O_2 measurements on a profiling float, J. Atmos. Ocean. Tech., 30, 112–126, doi:10.1175/JTECH-D-12-00043.1, 2013.

Fietzek, P., Fiedler, B., Steinhoff, T., and Körtzinger, A.: In situ quality assessment of a novel underwater pCO_2 sensor based on membrane equilibration and NDIR spectrometry, J. Atmos. Ocean. Tech., 31, 181–196, 2014.

Frieder, C. A., Gonzalez, J. P., Bockmon, E. E., Navarro, M. O., and Levin, L. A.: Can variable pH and low oxygen moderate ocean acidification outcomes for mussel larvae?, Glob. Chang. Biol., 20, 1–11, doi:10.1111/gcb.12485, 2013.

Garrard, S. L. and Beaumont, N. J.: The effect of ocean acidification on carbon storage and sequestration in seagrass beds; a global and UK context, Mar. Pollut. Bull., 86, 138–146, doi:10.1016/j.marpolbul.2014.07.032, 2014.

Gazeau, F., Borges, A. V., Barrón, C., Duarte, C. M., Iversen, N., Middelburg, J. J., Delille, B., Pizay, M., Frankignoulle, M., and Gattuso, J.: Net ecosystem metabolism in a micro-tidal estuary (Randers Fjord, Denmark): evaluation of methods, Mar. Ecol.-Prog. Ser., 301, 23–41, 2005.

Gazeau, F., Parker, L. M., Comeau, S., Gattuso, J.-P., O'Connor, W. A., Martin, S., Pörtner, H.-O., and Ross, P. M.: Impacts of ocean acidification on marine shelled molluscs, Mar. Biol., 160, 2207–2245, doi:10.1007/s00227-013-2219-3, 2013.

Hammer, K., Schneider, B., Kuliński, K., and Schulz-Bull, D. E.: Precision and accuracy of spectrophotometric pH measurements at environmental conditions in the Baltic Sea, Estuar. Coast. Shelf Sci., 146, 24–32, 2014.

Harvey, B. P., Gwynn-Jones, D., and Moore, P. J.: Meta-analysis reveals complex marine biological responses to the interactive effects of ocean acidification and warming, Ecol. Evol., 3, 1016–1030, doi:10.1002/ece3.516, 2013.

Herkül, K. and Kotta, J.: Effects of eelgrass (*Zostera marina*) canopy removal and sediment addition on sediment characteristics and benthic communities in the northern Baltic Sea, Mar. Ecol.-Evol. Persp., 30, 74–82, doi:10.1111/j.1439-0485.2009.00307.x, 2009.

Hiebenthal, C., Philipp, E. E. R., Eisenhauer, A., and Wahl, M.: Effects of seawater pCO_2 and temperature on shell growth, shell stability, condition and cellular stress of western Baltic Sea *Mytilus edulis* (L.) and *Arctica islandica* (L.), Mar. Biol., 160, 2073–2087, doi:10.1007/s00227-012-2080-9, 2013.

Hofmann, G. E., Smith, J. E., Johnson, K. S., Send, U., Levin, L. A., Micheli, F., Paytan, A., Price, N. N., Peterson, B., Takeshita, Y., Matson, P. G., Crook, E. D., Kroeker, K. J., Gambi, M. C., Rivest, E. B., Frieder, C. A., Yu, P. C., and Martz, T. R.: High-frequency dynamics of ocean pH: a multi-ecosystem comparison., PLoS One, 6, e28983, doi:10.1371/journal.pone.0028983, 2011.

Holmer, M. and Bondgaard, E. J.: Photosynthetic and growth response of eelgrass to low oxygen and high sulfide concentrations during hypoxic events, Aquat. Bot., 70, 29–83, 2001.

Invers, O., Romero, J., and Pérez, M.: Effects of pH on seagrass photosynthesis: a laboratory and field assessment, Aquat. Bot., 59, 185–194, doi:10.1016/S0304-3770(97)00072-7, 1997.

Jokumsen, A. and Fyhn, H. J.: The influence of aerial exposure upon respiratory and osmotic properties of haemolymph from two intertidal mussels, *Mytilus edulis* L., and *Modiolus modiolus* L., J. Exp. Mar. Biol. Ecol., 61, 189–203, doi:10.1016/0022-0981(82)90008-9, 1982.

Karez, R.: Kartierung mariner Pflanzenbestände im Flachwasser der Ostseeküste – Schwerpunkt *Fucus* und *Zostera*: Außenküste der schleswig-holsteinischen Ostsee und Schlei, Landesamt für Landwirtschaft, Umwelt und ländliche Räume, Flintbek, Germany, 2008.

Keeling, R. F., Körtzinger, A., and Gruber, N.: Ocean deoxygenation in a warming world, Ann. Rev. Mar. Sci., 2, 199–229, doi:10.1146/annurev.marine.010908.163855, 2010.

Kuliński, K., Schneider, B., Hammer, K., Machulik, U., and Schulz-Bull, D.: The influence of dissolved organic matter on the acid–base system of the Baltic Sea, J. Marine Syst., 132, 106–115, doi:10.1016/j.jmarsys.2014.01.011, 2014.

Lavigne, H. and Gattuso, J.-P.: seacarb: seawater carbonate chemistry with R, R package version 2.3. 3, Software available at: http://scholar.google.com/scholar?hl=en&btnG=Search&q=intitle:seacarb:+seawater+carbonate+chemistry+with+R.+R+package+version+2.3#0 (last access: 2015), 2010.

Melzner, F., Thomsen, J., Koeve, W., Oschlies, A., Gutowska, M. A., Bange, H. W., Hansen, H. P., and Körtzinger, A.: Future ocean acidification will be amplified by hypoxia in coastal habitats, Mar. Biol., 160, 1875–1888, doi:10.1007/s00227-012-1954-1, 2012.

Millero, F. J.: Carbonate constants for estuarine waters, Mar. Freshwater. Res., 61, 139–142, 2010.

Miloshevich, L. M., Paukkunen, A., Vömel, H., and Oltmans, S. J.: Development and validation of a time-lag correction for Vaisala radiosonde humidity measurements, J. Atmos. Ocean. Tech., 21, 1305–1327, 2004.

Newell, C. R., Short, F., Hoven, H., Healey, L., Panchang, V., and Cheng, G.: The dispersal dynamics of juvenile plantigrade mussels (*Mytilus edulis* L.) from eelgrass (*Zostera marina*) meadows in Maine, U.S.A., J. Exp. Mar. Biol. Ecol., 394, 45–52, doi:10.1016/j.jembe.2010.06.025, 2010.

Nightingale, P. D., Malin, G., Law, C. S., Watson, A. J., Liss, P. S., Liddicoat, M. I., Boutin, J., and Upstill-Goddard, R. C.: In situ evaluation of air–sea gas exchange parameterizations using novel conservative and volatile tracers, Global Biogeochem. Cy., 14, 373–387, available at: http://lgmacweb.env.uea.ac.uk/ajw/Reprints/Nightingale_et_al_GBC_2000.pdf (last access: 29 January 2013), 2000.

NOAA – ESRL, available at: http://www.esrl.noaa.gov/gmd/ccgg/trends (last access: 2014), 2014.

Odum, H. T.: Primary production in flowing waters, Limnol. Oceanogr., 1, 102–117, 1956.

Perez, F. F. and Fraga, F.: The pH measurements in seawater on the NBS scale, Mar. Chem., 21, 315–327, 1987.

Peterson, B. J. and Heck, K. L.: Positive interactions between suspension-feeding bivalves and seagrass – a facultative mutualism, Mar. Ecol.-Prog. Ser., 213, 143–155, doi:10.3354/meps213143, 2001.

Pörtner, H.: Ecosystem effects of ocean acidification in times of ocean warming: a physiologist's view, Mar. Ecol.-Prog. Ser., 373, 203–217, doi:10.3354/meps07768, 2008.

Raun, A. L. and Borum, J.: Combined impact of water column oxygen and temperature on internal oxygen status and growth of *Zostera marina* seedlings and adult shoots, J. Exp. Mar. Biol. Ecol., 441, 16–22, doi:10.1016/j.jembe.2013.01.014, 2013.

Reusch, T. B. H.: Factors Structuring the *Mytilus*- and *Zostera*-Community in the Western Baltic: an Experimental Approach, Christian Albrechts University of Kiel, Kiel, Germany, 1994.

Reusch, T. B. H.: Differing effects of eelgrass *Zostera marina* on recruitment and growth of associated blue mussels *Mytilus edulis*, Mar. Ecol.-Prog. Ser., 167, 149–153, doi:10.3354/meps167149, 1998.

Reusch, T. B. H. and Chapman, A. R. O.: Storm effects on eelgrass (*Zostera marina* L.) and blue mussel (*Mytilus edulis* L.) beds, J. Exp. Mar. Biol. Ecol., 192, 257–271, doi:10.1016/0022-0981(95)00074-2, 1995.

Saderne, V., Fietzek, P., and Herman, P. M. J.: Extreme variations of pCO_2 and pH in a macrophyte meadow of the Baltic Sea in summer: evidence of the effect of photosynthesis and local upwelling, PLoS One, 8, e62689, doi:10.1371/journal.pone.0062689, 2013.

Sanders, T., Widdicombe, S., Calder-Potts, R., and Spicer, J. I.: Environmental hypoxia but not minor shell damage affects scope for growth and body condition in the blue mussel *Mytilus edulis* (L.), Mar. Environ. Res., 95, 74–80, doi:10.1016/j.marenvres.2013.12.013, 2014.

Soetaert, K.: Using R for scientific computing, available at: http://citeseerx.ist.psu.edu/viewdoc/summary?doi=10.1.1.167.9844 (last access: 2015), 2008.

Sommer, U., Meusel, B., and Stielau, C.: An experimental analysis of the importance of body-size in the seastar–mussel predator–prey relationship, Acta Oecol., 20, 81–86, doi:10.1016/S1146-609X(99)80019-8, 1999.

Thomsen, J., Gutowska, M. A., Saphörster, J., Heinemann, A., Trübenbach, K., Fietzke, J., Hiebenthal, C., Eisenhauer, A., Körtzinger, A., Wahl, M., and Melzner, F.: Calcifying invertebrates succeed in a naturally CO_2-rich coastal habitat but are threatened by high levels of future acidification, Biogeosciences, 7, 3879–3891, doi:10.5194/bg-7-3879-2010, 2010.

Thomsen, J., Haynert, K., Wegner, K. M., and Melzner, F.: Impact of seawater carbonate chemistry on the calcification of marine bivalves, Biogeosciences Discuss., 12, 1543–1571, doi:10.5194/bgd-12-1543-2015, 2015.

Tyrrell, T., Schneider, B., Charalampopoulou, A., and Riebesell, U.: Coccolithophores and calcite saturation state in the Baltic and Black Seas, Biogeosciences, 5, 485–494, doi:10.5194/bg-5-485-2008, 2008.

Vaquer-Sunyer, R. and Duarte, C. M.: Thresholds of hypoxia for marine biodiversity, P. Natl. Acad. Sci. USA, 105, 15452–15457, doi:10.1073/pnas.0803833105, 2008.

Vinther, H. F. and Holmer, M.: Experimental test of biodeposition and ammonium excretion from blue mussels (*Mytilus edulis*) on eelgrass (*Zostera marina*) performance, J. Exp. Mar. Biol. Ecol., 364, 72–79, doi:10.1016/j.jembe.2008.07.003, 2008.

Vinther, H. F., Laursen, J. S., and Holmer, M.: Negative effects of blue mussel (*Mytilus edulis*) presence in eelgrass (*Zostera marina*) beds in Flensborg Fjord, Denmark, Estuar. Coast. Shelf S., 77, 91–103, doi:10.1016/j.ecss.2007.09.007, 2008.

Vinther, H. F., Norling, P., Kristensen, P., Dolmer, P., and Holmer, M.: Effects of coexistence between the blue mussel and eelgrass on sediment biogeochemistry and plant performance, Mar. Ecol.-Prog. Ser., 447, 139–149, doi:10.3354/meps09505, 2012.

Waldbusser, G. G., Hales, B., Langdon, C. J., Haley, B. A., Schrader, P., Brunner, E. L., Gray, M. W., Miller, C. A., and Gimenez, I.: Saturation-state sensitivity of marine bivalve larvae to ocean acidification, Nature Climate Change, 5, 273–280, doi:10.1038/nclimate2479, 2014.

Wang, W. and Widdows, J.: Metabolic responses of the common mussel *Mytilus edulis* to hypoxia and anoxia, Mar. Ecol.-Prog. Ser., 95, 205–214, doi:10.3354/meps095205, 1993.

Wang, W. X., Widdows, J., and Page, D. S.: Effects of organic toxicants on the anoxic energy metabolism of the mussel *Mytilus edulis*, Marine Environ. Res., 34, 327–331., 1992.

Table 1. Summary (mean ± SD) of the daily means, minimal and maximal values and amplitude of variations for O_2 and different parameters of the carbonate chemistry in August (n = 20 days) and September (n = 25 days).

	O_2 mmol kg^{-1}	pCO_2 µatm	DIC µmol kg^{-1}	CO_3^{2-} µmol kg^{-1}	pH_T
August					
Mean	237 ± 18	628 ± 115	1891 ± 32	87 ± 11	7.938 ± 0.068
Min.	176 ± 22	291 ± 74	1798 ± 38	52 ± 16	7.665 ± 0.116
Max.	315 ± 33	1171 ± 314	1964 ± 46	139 ± 30	8.212 ± 0.095
Amplitude	139 ± 41	880 ± 327	166 ± 54	87 ± 39	0.547 ± 0.159
September					
Mean	190 ± 32	649 ± 193	1877 ± 60	75 ± 14	7.915 ± 0.111
Min.	141 ± 31	348 ± 123	1808 ± 72	45 ± 12	7.688 ± 0.129
Max.	251 ± 37	1085 ± 343	1937 ± 55	116 ± 25	8.145 ± 0.126
Amplitude	110 ± 28	737 ± 281	129 ± 36	71 ± 23	0.457 ± 0.121

Table 2. Summary statistics for the salinity to TA regressions, from discrete samples, used for the modelling of the TA time series in August (n = 14 samples) and September (n = 16 samples).

	Ω_{arag}	Ω_{calc}
August		
Mean	1.4 ± 0.2	2.4 ± 0.3
Min.	0.7 ± 0.2	1.3 ± 0.3
Max.	2.3 ± 0.5	3.9 ± 0.8
Amplitude	1.6 ± 0.5	2.7 ± 0.9
Undersat. time (h d^{-1})	5.7 ± 4.0	0.4 ± 0.8
September		
mean	1.2 ± 0.2	2.0 ± 0.4
Min.	0.7 ± 0.2	1.2 ± 0.3
Max.	1.9 ± 0.4	3.1 ± 0.7
Amplitude	1.1 ± 0.4	1.9 ± 0.6
Undersat. time (h d^{-1})	8.8 ± 6.3	1.3 ± 2.4

Table 3. summary (mean ± SD) of the daily means, minimal and maximal values and amplitude of variations and duration of undersaturation condition per day for in August (n = 20 days) and September (n = 25 days).

	August	September
Slope	40.0	44.1
Slope p value	< 0.001	< 0.001
Intercept	1349.2	1248.9
Intercept p value	< 0.001	< 0.001
Df	11	15
F-statistic	22.42	211.5
Regression p value	< 0.001	< 0.001
R^2	0.67	0.93
Residuals standard deviation (µmol TA kg^{-1})	13.4	12.3

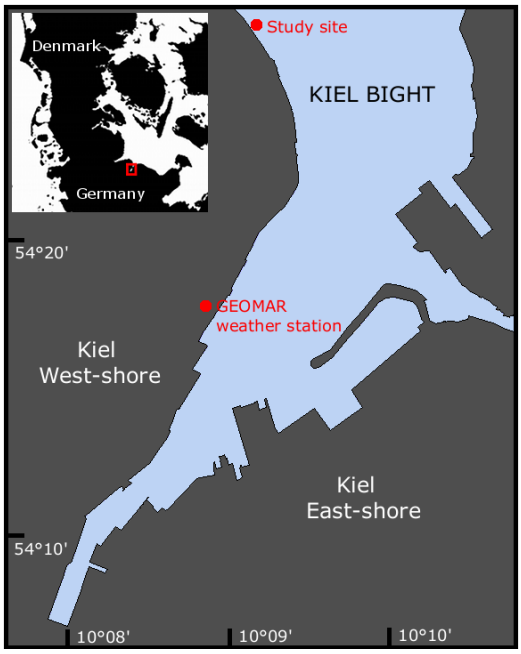

Figure 1. Map of the Kiel Bight with study site and the GEOMAR highlighted as well as a larger scale map for orientation as an inlay.

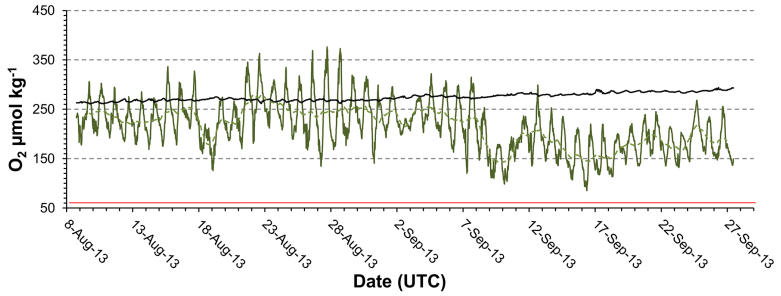

Figure 2. Time-series of dissolved oxygen concentration at 10 min measurement interval (solid green line) and as 24 h moving average (dashed green line). Also shown is the oxygen saturation concentration calculated from the water temperature and salinity (black). The red line represents the hypoxia threshold of 60 µmol kg^{-1}.

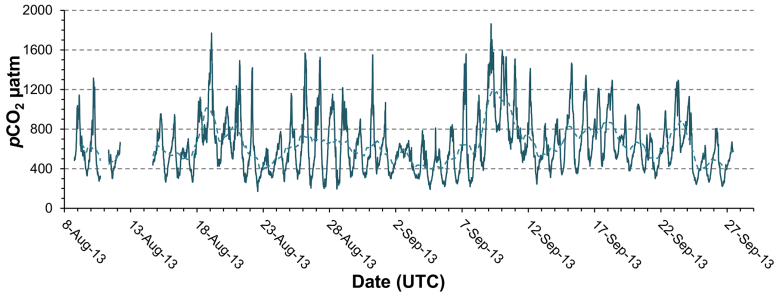

Figure 3. Time-series of pCO_2 at 1 min measurement interval (solid line) and 24 h moving average (dashed line).

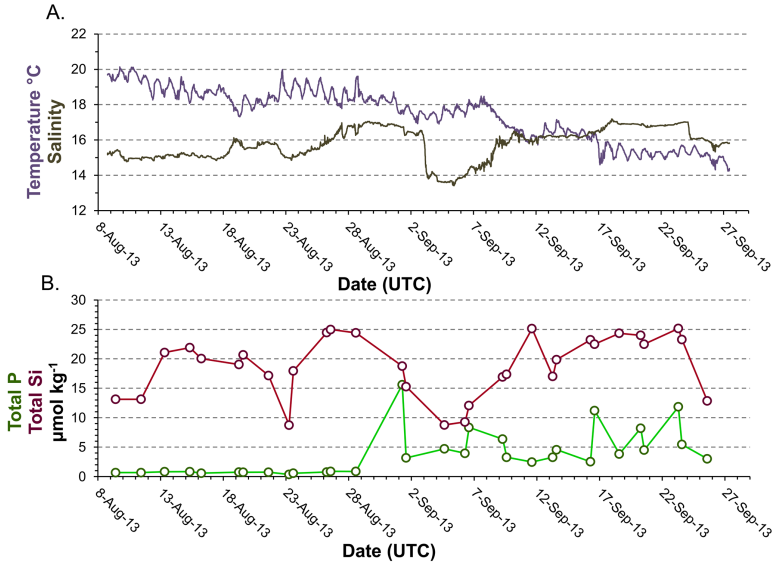

Figure 4. (a) Salinity and temperature (10 min sampling interval). **(b)** Total phosphate (green) and silicate (red) concentration from the 31 discrete sampling events at the sensors' location.

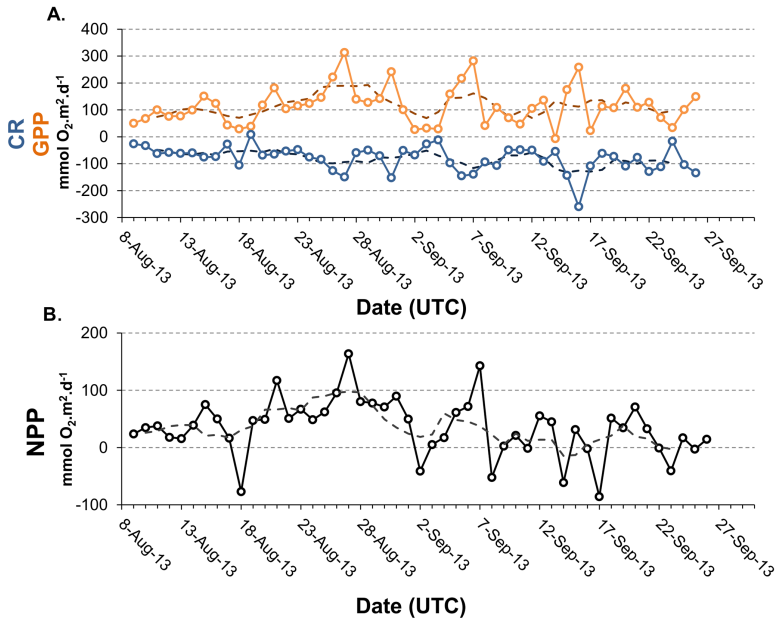

Figure 5. (a) Gross primary production (GPP, orange solid line) as the integral of the fluxes of O_2 at daytime extended to 24 h after correction for the air–sea exchanges of O_2. Community respiration (CR, blue solid line) is the integral at nighttime, extended to 24 h, after air sea exchange of O_2. **(b)** Net primary production (NPP) as the difference between CR and GPP. Dashed lines represent 7 days running averages.

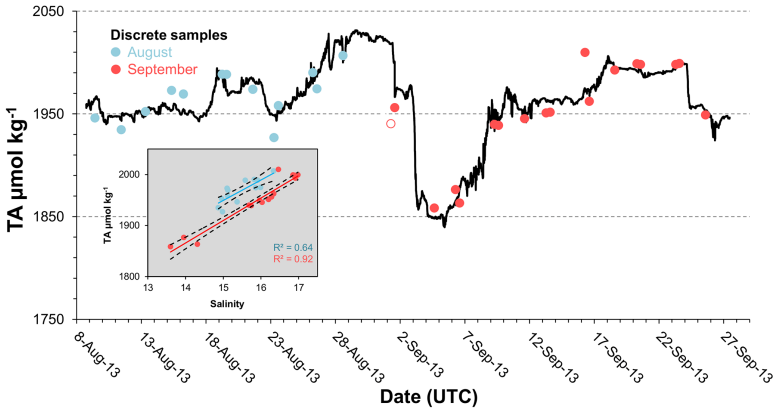

Figure 6. Small panel: linear regressions Total alkalinity (TA) as function of salinity in discrete samples for the months of August in blue (n = 14) and September in red (n = 16), see Table 3 for equations and statistics. Dashed lines are 90 % confidence intervals. Main panel: TA time series calculated from salinity using the regression equations from August and September. Dots are the TA in the 31 discrete samples used for the regressions. The sample from the 01 September at 06:40 LT (no fill) was not considered for the regressions.

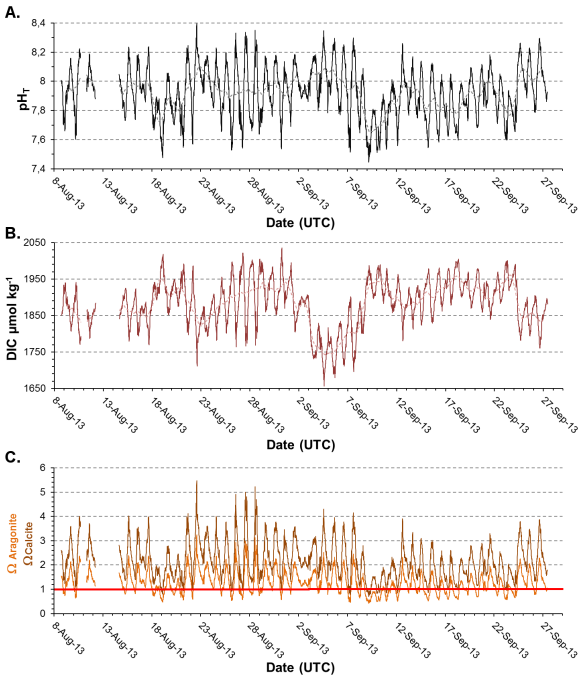

Figure 7. (a) pH in total scale and **(b)** dissolved inorganic carbon (DIC) calculated from total alkalinity and pCO_2 (10 min interval). Dashed lines are 24 h moving average. **(c)** Saturation states for aragonite (Ω aragonite, light brown) and calcite (Ω calcite, dark brown) calculated from total alkalinity and pCO_2 (10 min interval). The red line represent the dissolution threshold Ω = 1.

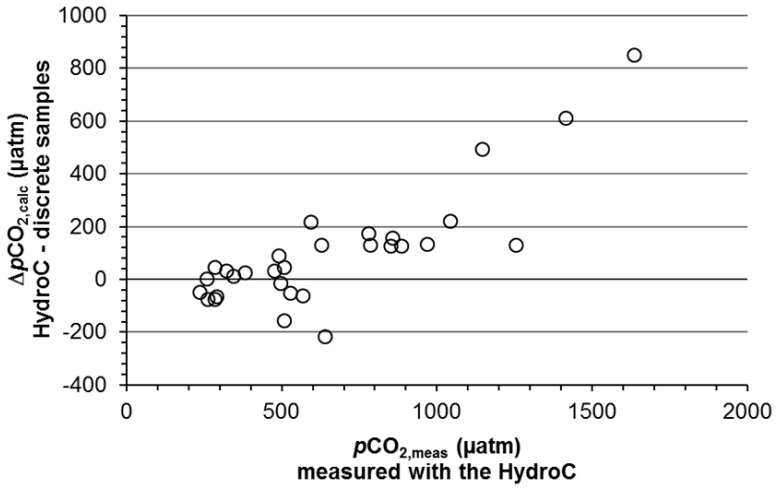

Figure 8. Inconsistencies found within the carbonate system calculations. The pCO_2 as measured by the HydroC™ shows significantly larger values than the pCO_2 derived from DIC and TA in discrete samples. A small number of samples at high pCO_2, HydroC™ greater than ~ 1100 µatm are striking.

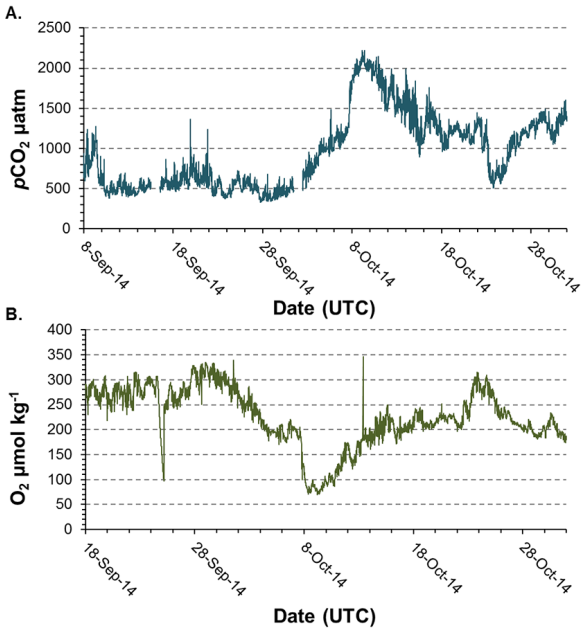

Figure 9. (a) pCO_2 (5 min sampling interval); **(b)** O_2 (10 min sampling interval) from pelagic mooring of the HydroC™ sensor at the GEOMAR Pier at 1 m depth in summer/fall 2014 displaying large upwelling events.

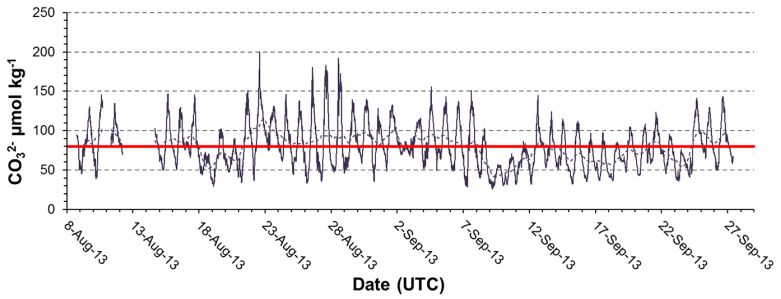

Figure 10. Carbonate ion concentration calculated from total alkalinity and pCO_2 (10 min interval). Dashed line is the 24 h moving average. The red line represents the threshold of 80 µmol kg^{-1} below which calcification declines in mussels according to Thomsen et al. (2015).